ACS OMEGA

Open Access

http://pubs.acs.org/journal/acsodf

Article

High-Titer Recombinant Adenovirus 26 Vector GMP Manufacturing in HEK 293 Cells with a Stirred Single-Use Bioreactor for COVID-19 Vaccination Purposes

Hossein Sedighikamal,* Alireza Sattarzadeh, Reza Karimi Mostofi, Behnoush Dinarvand, and Madineh Nazarpour

Cite This: *ACS Omega* 2023, 8, 36720−36728

Read Online

ACCESS | Metrics & More | Article Recommendations

ABSTRACT: The severe acute respiratory syndrome coronavirus 2 (SARS-CoV-2 virus) pandemic has shown the importance of pursuing various vaccine manufacturing strategies. In the present study, the HEK 293 cells were infected with recombinant adenovirus serotype 26 (rAd26), and the effects of critical process parameters (CPPs) including viable cell density (VCD) at infection time (0.5×10^6, 0.8×10^6, 1.4×10^6, 1.8×10^6, and 2.5×10^6 cells/mL), the multiplicity of infection (MOI) = 3, 6, 9, 12, and 15, and two aeration strategies (high-speed agitation with a sparging system and low-speed agitation with an overlay system) were investigated experimentally. The results of small-scale experiments in 2 L shake flasks (SF 2L) demonstrated that the initial VCD and MOI could affect the cell proliferation and viability. The results at these experiments showed that VCD = 1.4×10^6 cells/mL and MOI = 9 yielded $TCID_{50}$ /mL = $10^{8.9}$, at 72 h post-infection (hpi), while the virus titer at VCD = 0.5×10^6 and 0.8×10^6 cells/mL was lower compared to that of VCD = 1.4×10^6 cells/mL. Moreover, our findings showed that VCDs > 1.8×10^6 cells/m with MOI = 9 did not have a positive effect on $TCID_{50}$ /mL and MOI = 3 and 6 were less efficient, whereas MOI > 12 decreased the viability drastically. In the next step, the optimized CPPs in a small scale were exploited in a 200 L single-use bioreactor (SUB), with good manufacturing practice (GMP) conditions, at RPM = 25 with an overlay system, yielding high-titer rAd26 manufacturing, i.e., $TCID_{50}$/mL = $10^{8.9}$, at 72 hpi.

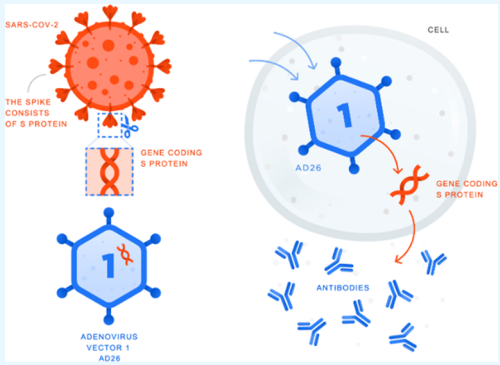

1. INTRODUCTION

The syndrome coronavirus 2 (SARS-CoV-2) caused coronavirus 2019 (COVID-19), which has posed a serious threat to public health. On March 2020, the World Health Organization (WHO) proclaimed the SARS-CoV-2 virus a global pandemic and gave the virus the COVID-19 designation.[1] The SARS-CoV-2 virus is classified as a β coronavirus, which is a member of the Coronaviridae family.[2,3] Given that the SARS-CoV-2 virus can spread easily from infected individuals without showing symptoms, it is a challenging issue to manage this pandemic without any global vaccination strategy.[4] For this reason, global priority is the development and enhancement of different vaccine platforms against this viral infection.[5] Several developed vaccines get emergency use authorization (EUA) for the COVID-19 pandemic. These new vaccine platforms use a variety of technologies, including viral vectors, mRNA-based, and protein subunits, compared to traditional techniques like the inactivated virus vaccines.[6]

Adenovirus has been applied for vaccine development purposes due to high safety and its promising efficacy in stimulation of both cellular and humoral immunity.[7,8] Chavda et al. declared that the immune response elicited by such vaccines is comparatively higher than other approved vaccine candidates that require a booster dose to provide sufficient immune protection and also have current cGMP-friendly processes.[9] Currently, different adenovirus serotypes are used as a platform for vaccine candidates. Adenovirus serotype 5 (Ad5) is the most thoroughly researched due to its early isolation, efficient reverse genetic system, good candidate for gene therapy, and vaccine vector applications.[10] On the other hand, adenovirus serotype 26 (Ad26) was recently examined for its potential use as a vector with a lower seroprevalence for gene-based vaccinations and oncolytic viral therapy.[11,12] Ad26 also shows favorable thermal stability profiles at a storage temperature of −20 °C, compatible with existing cold supply chains compared to mRNA-based vaccines, which unpleasantly

Received: May 2, 2023
Accepted: September 14, 2023
Published: October 2, 2023

need to be shipped and stored at deep freeze conditions (−80 °C).[13] Moreover, Ad26-based vaccines record a successful experience in the prevention of life-threatening viruses, such as Ebola.

Sputnik is an adenovirus viral vector vaccine for COVID-19 (developed by Gamaleya, Russia) and is the world's first registered vector vaccine for the prevention of COVID-19. This vaccine can be formulated in two techniques: as a ready-to-use solution in water that is frozen at the common freezer storage temperature (<−18 °C) and as a freeze-dried (lyophilized) powder, which can be stored at 2−8 °C. The freeze-dried powder needs to be reconstituted with sterile water for injection (WFI) before administration.[14] The lyophilized formulation is similar to the smallpox vaccine, avoiding the need for continuous cold-chain storage—as a vital accessory for mRNA-based vaccines (the Pfizer−BioNTech and Moderna)—and letting transportation to remote locations with a reduced risk of degradation.[15,16]

The effectiveness of COVID-19 vaccines or any other vaccine is firmed in mass vaccination in a real-world setting (not in clinical trials). This is a valuation of how well the vaccine protects people from outcomes such as infection, symptomatic illness, hospitalization, and death. The effectiveness is evaluated outside of clinical trials, which by contrast evaluate the efficacy of the vaccine.[17,18] A vaccine is generally considered effective if the estimate is ≥50% with a > 30% lower limit of the 95% confidence interval (CI).[19] Effectiveness is generally expected to slowly decrease over time, and the WHO recommends that successful vaccines should show an estimated risk reduction of at least half, with sufficient precision to conclude that the true vaccine efficacy is greater than 30%. This means that the 95% CI for the trial result should exclude efficacy less than 30%. The current US Food and Drug Administration (FDA) guidance includes this lower limit of 30% as a criterion for vaccine licensure.[20]

Various processes for bulk manufacturing of viral-based vaccines were presented, for example, three strains of H1N1, H3N2, and influenza B vaccines were cultured in Cytodex microcarriers,[21] fed-batch culture,[22] and perfusion bioreactor equipped with a spin filter, respectively,[23,24] and influenza A virus was expanded in the perfusion bioreactor using an alternating tangential flow (ATF).[25] Also, disposable fixed-bed bioreactors have been used in the adherent cell culture technique to produce a higher yield of live viruses[26,27] and there are various studies showing a comparable cell growth rate and virus production yield for disposable and stainless-steel bioreactors.[28] Cell culture-based vaccine production employing bioreactors has expanded manufacturing capacities and facilitated improved process control, while ensuring the product quality. Technology based on cell culture gives producers the ability to adapt to market requirements more rapidly with shorter production cycles. In addition, cell culture-based viruses are more similar to the circulating strains than the viruses produced in eggs as hosts, which may contain antigenic variations.[29] The human embryonic kidney (HEK) 293 cell lines have been commonly used over the last decades, not only for the basic research such as protein interaction and signal transduction studies but also for the GMP manufacturing of recombinant proteins and viral vectors in the biopharmaceutical industry owing to the high transfectivity, acceptable growth rate, and human-like post-translation modifications.[30−33] For this cell line, the results showed that the host cell passage number, ratio of the number of virus particles to each cell (i.e., multiplicity of infection (MOI)), viable cell density (VCD), viral stock passage number, contact time of the adenoviral vector with the host cells during culture, and host cell viability during infection are all critical factors that affect a successful infection.[2,3,34] Previous studies have also declared that addition of fresh culture medium at the time of infection (ToI) or the feeding strategies (with glucose or amino acids) at 24 h post-infection (hpi) together with pH controlling within the optimal ranges allowed a high rAd productivity at VCD = 2−3 × 10^6 cells/mL.[35,36]

Besides, it was found that the optimal process parameters (agitation speed, aeration, pH, dissolved oxygen concentration, medium composition, temperature, etc.) strongly affect cell growth and virus replication as well. The process optimization and scale up in stirred single-use bioreactors (SUBs) require the identification of critical parameters because the use of agitation and aeration increases the shear stress sensed by cells and thus increases the risk of cell damage, resulting in the product yield reduction. The critical process parameters (CPPs) including dissolved oxygen (DO), pH level, cell culture osmolality, temperature, agitation speed, and aeration system must be carefully investigated during process optimization. In this study, the effects of CPPs including VCD (= 0.5 × 10^6, 0.8 × 10^6, 1.4 × 10^6 and 1.8 × 10^6 and 2.5 × 10^6 cells/mL) at ToI, the MOI (3, 6, 9, 12, and 15), and hpi (0−120 h) on rAd26 GMP manufacturing were experimentally studied, using a one-factor-at-a-time (OFAT) approach. Initially, the effects of VCD at ToI, MOI, and the viability were investigated in 2 L shake flasks (SFs 2 L) on the rAd26 virus titer using a batch-mode cell culture. Subsequently, the optimum CPPs were exploited to scale up the rAd26 GMP manufacturing up to 200 L in SUB. In the next steps, the effect of agitation (low-speed agitation at RPM = 25 and high-speed agitation at RPM = 80) and aeration system (with sparging and without sparging, i.e., through overlay only) was examined in 200 L SUB.

2. MATERIALS AND METHODS

2.1. Cell Line and Culture Medium. In order to manufacture the recombinant adenovirus rAd26-S-CoV-2 (Gamaleya Institute, Russia) containing the recombinant SARS-CoV-2 Spike glycoprotein gene, HyClone (Cytiva) serum-free medium (SFM) was used as the basal media. HEK 293 cells that constitutively express the E1 proteins (necessary for viral replication) were grown from a working cell bank (WCB) and scaled up from initial 2 L shaker flasks (SF) to 200 L bioreactors. For this purpose, a WCB vial containing 10 × 10^6 cells/mL of viable HEK 293 cells was thawed in a T-flask 75 (Thermo Scientific) containing 20 mL of prewarmed HyClone SFM and incubated at 37 °C under 5% CO_2 to prepare the seed for the next step of cultivation. The HEK 293 cells cultivated in the T-flasks were then inoculated into the next step after 3−5 days (SF 250 mL (Corning), with a final volume of 80 mL). All cell suspensions were incubated in a shaker incubator (Kuhner, Switzerland) at 37 °C and RPM = 90, with 5% CO_2. The subcultures then were transferred to SF 2 L with a working volume of 600 mL. In all steps, cell counting, viability, and morphology were monitored daily with an inverted microscope under a Neubauer hemocytometry chamber.

2.2. Adenovirus rAd26 Stock Preparation. The rAd26-S-CoV-2 virus was used to infect the suspension of HEK 293 host cells (Gamaleya Institute, Russia). The virus stock used

https://doi.org/10.1021/acsomega.3c03007
ACS Omega 2023, 8, 36720−36728

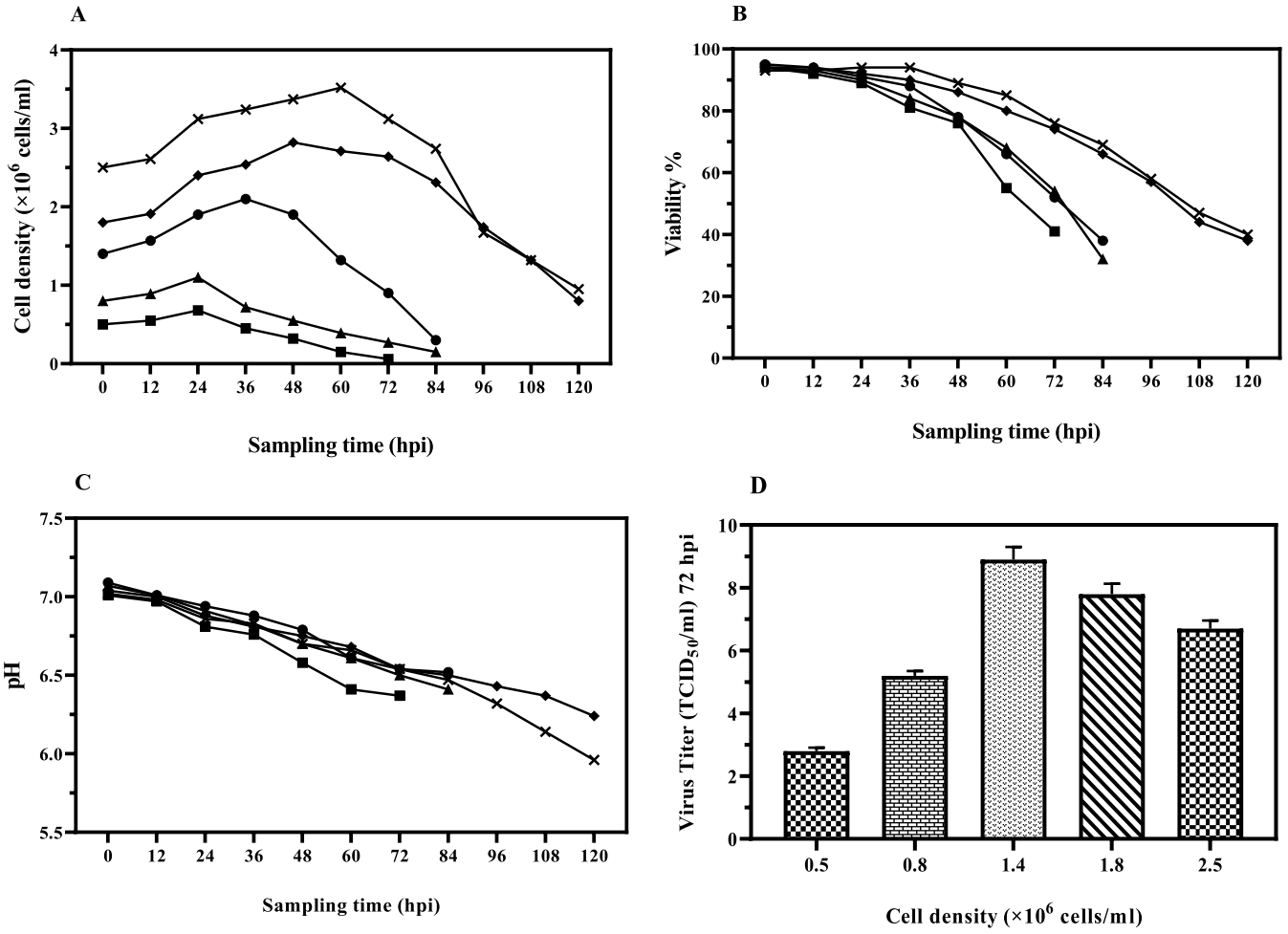

Figure 1. Time profiles of initial VCD on the cell growth curve (A), viability (B), pH trend after infection (C), and adenovirus rAd26 production viral titer 72 h after infection (D) by HEK293 cells at an MOI = 9 in 2 L shaker flask cultures. ■: VCD = 0.5 × 10^6 cells/mL; ▲: VCD = 0.8 × 10^6 cells/mL; ●: VCD = 1.4 × 10^6 cells/mL; ♦: VCD = 1.8 × 10^6 cells/mL; and ×: VCD = 2.5 × 10^6 cells/L. All results are the mean values of triplicate data.

for all experiments was prepared by infecting HEK 293 cells at VCD = 1.4 × 10^6 cells/mL in SF 2 L with MOI = 9. All the cultures were incubated at 37 °C in 5% CO_2 and orbital shaking RPM = 90. After 120 hpi, the sample was taken from the SF 2 L for cell counting and to calculate the virus stock necessary for infection, considering the MOI = 9. After harvesting the infected HEK 293 cells at 120 hpi, they were lysed mechanically (without adding any chemical component) using freeze−thaw cycles (by three cycles of freezing at −80 °C and then thawing in a water bath at 37 °C) to release the adenoviral vectors from the HEK 293 cytoplasm. The lysate was filtered using a sterile 0.22 μm poly(ether sulfone) (PES) membrane filter (3M) to remove the cell debris and then was aliquoted into sterile containers and stored at −80 °C for virus stock purposes in the next steps.

2.3. Cell Growth and Infection in a 50 L Wave SUB. To expand the cell culture and prepare the virus stock required in a 200 L SUB (Sartorius, Germany), ∼10 L of SFM was aseptically transferred into a 50 L wave SUB (Sartorius, Germany) through a sterile port of the cell culture bag. The SUB parameters were set as temperature = 37 ± 0.5 °C and 5% CO_2, agitation rate = 20 ± 2 rpm, angle = 7°, pH = 7.0 ± 0.2, and DO = 35 ± 5%. In the 50 L wave SUB, the HEK 293 cells were subcultured/infected same as the method described for the SF 2 L. The VCD and viability were monitored daily, and once the VCD reached 3−3.5 × 10^6 cells/mL, the cell was subcultured again in the next step, to expand the cells for the final volume in a 200 L SUB.

2.4. Cell Expansion and Infection in a 200 L SUB. The virus stock to infect the 200 L SUB was prepared as previously described for SFs and then in the wave SUB. The 200 L stirred SUB was initially run with the cultivation of ∼40 L SFM with conditions including pH = 7.10 ± 0.05, agitation = 25 ± 1 rpm, and temperature = 37 ± 0.1 °C to perform the medium hold for 24 h (to check the medium sterility for any microbial contamination). Then, the cells were transferred to the bioreactor at the initial VCD = 0.5−0.8 × 10^6 cells/mL. The fermentation was done in fed-batch mode, and once the VCD reached ≥2.50 ± 0.1 × 10^6 cells/mL, the cell suspension was diluted four times, i.e., 120 L of culture medium was aseptically added into the bioreactor with a flow rate of ∼1 L/min, using a peristaltic pump (Watson Marlow 520, United Kingdom). The agitation was set to RPM = 40, and once the VCD reached 1.4 ± 0.1 × 10^6 cells/mL (on the third day), the cells were then infected with the virus stock with MOI = 9. Feeding with glucose (concentration of 45% w/v) was added after infection of the cells in the bioreactor to reach the final concentration of glucose to 0.30% w/v. Samples were taken daily from the

https://doi.org/10.1021/acsomega.3c03007
ACS Omega 2023, 8, 36720−36728

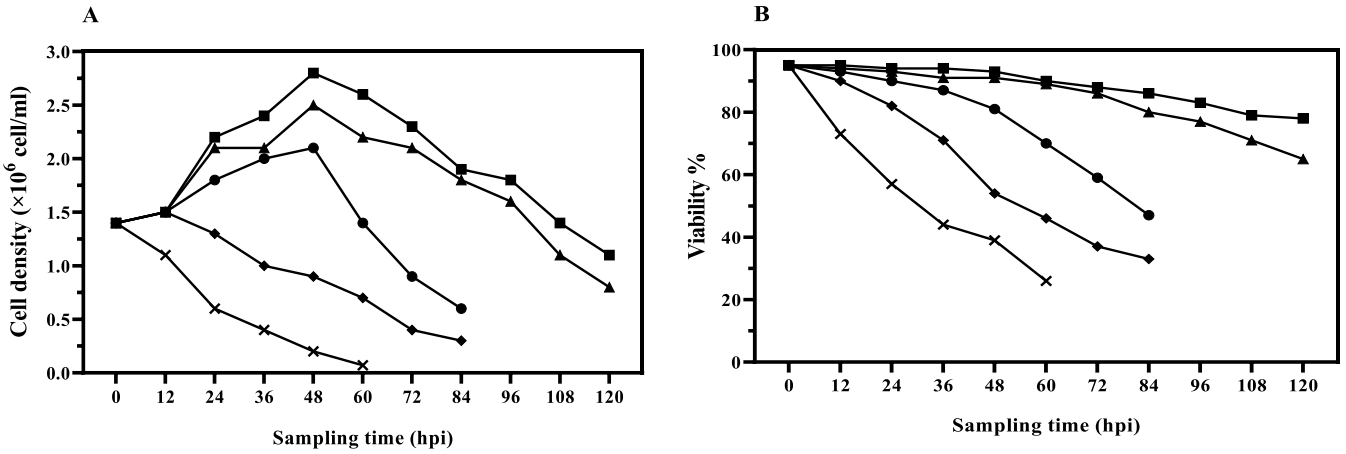

Figure 2. Effect of cell infection with different MOIs on cell density (A) and viability % (B). In all experiments, the HEK293 cells at VCD = 1.4 × 10^6 cells/mL in SF 2 L were infected. ■: MOI = 3; ▲: MOI = 6; ●: MOI = 9; ♦: MOI = 12, and ×: MOI = 15. All results are the mean values of triplicate data.

bioreactor to record VCD, cell viability, and pH. Also, at 72 hpi, the virus titer was quantified using $TCID_{50}$ assay. The aeration was done either through a sparger or overlay to control DO to keep within the optimal range (DO = 40 ± 10%) with pure oxygen.

2.5. Downstream Process. Following the upstream process, the chemical lysis was initiated at 72 hpi, by addition of lysis buffer (at a final concentration of 0.5% v/v Tween 20), the multistep downstream process including enzymatic endonuclease digestion was performed as previously described by Fedosyuk et al. to reduce host cell DNA, followed by depth filter clarification, initial concentration, and diafiltration by tangential flow filtration (TFF) with cutoff = 300 kDa (Millipore) and two-step chromatographic steps including anion exchange (AEX) and cation exchange (CEX) and finally formulating the drug substance.[37,38]

2.6. $TCID_{50}$ Assay. The number of infectious virus particles is frequently quantified using the median tissue culture infectious dose ($TCID_{50}$) assay.[39,40] This assay was performed on A549 cells (a human lung cancer epithelial cell line) and revealed by crystal violet staining, and then, the wells were observed and scored for the presence or absence of the cytopathic effect (CPE). Briefly, A549 cells were seeded at a cell density of 8 × 10^5 cells/mL in 96-well plates for 14 days, at 37 °C with CO_2. Tenfold serial dilutions of the viral sample were added to each well in quadruplicate (50 μL/well). After that, the number of wells with the CPE for each viral sample was determined (CPE was considered positive when more than 70% of the cells were compromised).[38] In this study, the $TCID_{50}$/mL factor was quantified using the TCID calculator (Marco binder, University of Heidelberg) based on the Spearman−Kalbur method.[41]

2.7. Statistical Analysis. Data pertaining to different periods were analyzed as repeated measures using the MIXED procedure of the statistical analysis system (SAS)[42] with a model containing the continuous effect of covariate (as a measure of the same variable), the random effect of cells, and the fixed effects of two types of agitation, VCD, and the MOI. By the use of Akaike's information criterion, the best covariance structure was specified among first-order autoregressive, unstructured, and compound symmetries. All data represent the mean values of three replicates.

3. RESULTS AND DISCUSSION

3.1. Effect of the Initial Cell Density on rAd26 Manufacturing. Figure 1 presents the results related to the cultivation of HEK 293 cells in SF 2 L, with a working volume of 600 mL, on a laboratorial scale, carried out at MOI = 9 and different initial VCDs. Figure 1A shows the infected HEK 293 cell density by hpi time. As can be seen, when the cultivation started with an initial VCD less than 1.4 × 10^6 cells/mL, before the cells had enough opportunity to duplicate, they have premature death in a way that going through the logarithmic phase and reaching a cell density higher than 0.8 × 10^6 and 1.0 × 10^6 cells/mL, respectively, were not observed. On the other hand, in the initial VCD = 1.8 and 2.5 × 10^6 cells/mL, they reached its maximum density, which is 2.5 × 10^6 and 3.5 × 10^6 cells/mL, respectively, at 48 and 60 hpi. By comparing the trend of changes in the viability of these cultures in Figure 1B, it can be understood that the viability of the infected cells follows almost the same trend of culture with VCDs = 0.5 × 10^6, 0.8 × 10^6, and 1.4 × 10^6 cells/mL; therefore, in the time window of 72−84 hpi, the viability in these three experiments is less than 40%. This is while for other cultivations in the same time period, the viability rate is higher than 70%. In Figure 1C that reports the rate of pH change in terms of hpi, as can be seen during the first 12 h, the pH value in all flasks had a similar decreasing trend; the culture with an initial VCD = 0.5 × 10^6 cells/mL has experienced a greater decrease in pH rather than the others, so that at a time of 60 hpi, the pH has decreased to around 6.30, while for other experiments, it is around 6.75. According to what is observed from Figure 1D, the highest virus titer was found in the SF infected with initial VCD = 1.4 × 10^6 cells/mL, so that the $TCID_{50}$/mL value was $10^{8.9}$ at 72 hpi. Due to the improved titer that was achieved in this flask, it is assumed that the viral titer was more productive in this cell density. After 48 hpi, the viability of the culture with initial VCD = 1.8 × 10^6 cells/mL fell out of 80% and the $TCID_{50}$/mL = $10^{7.8}$ was obtained, approximately 1.14-fold lower titer than what was observed with initial VCD = 1.4 × 10^6 cell/mL. Also, the flask with initial VCD = 2.5 × 10^6 cells showed $TCID_{50}$/mL = $10^{6.7}$, which was a lower titer compared to the flask with initial VCD = 1.8 × 10^6 cells/mL.

These results are in disagreement with the report, which indicated that the rAd yield could be increased with higher VCD at the time of infection and the optimum VCC = 1.04 ×

https://doi.org/10.1021/acsomega.3c03007
ACS Omega 2023, 8, 36720−36728

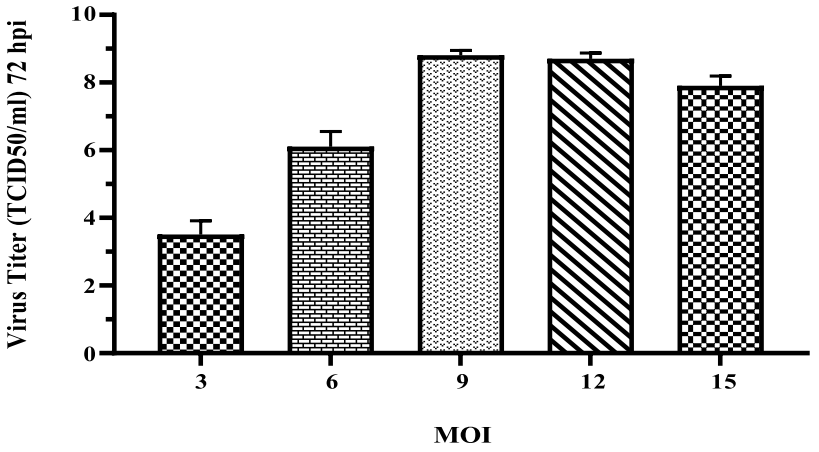

Figure 3. Effect of different MOIs on rAd26 titer at VCD = 1.4 × 10^6 cells/mL and 72 hpi in 2 L shaker flask cultures. Results are the mean values of triplicate data.

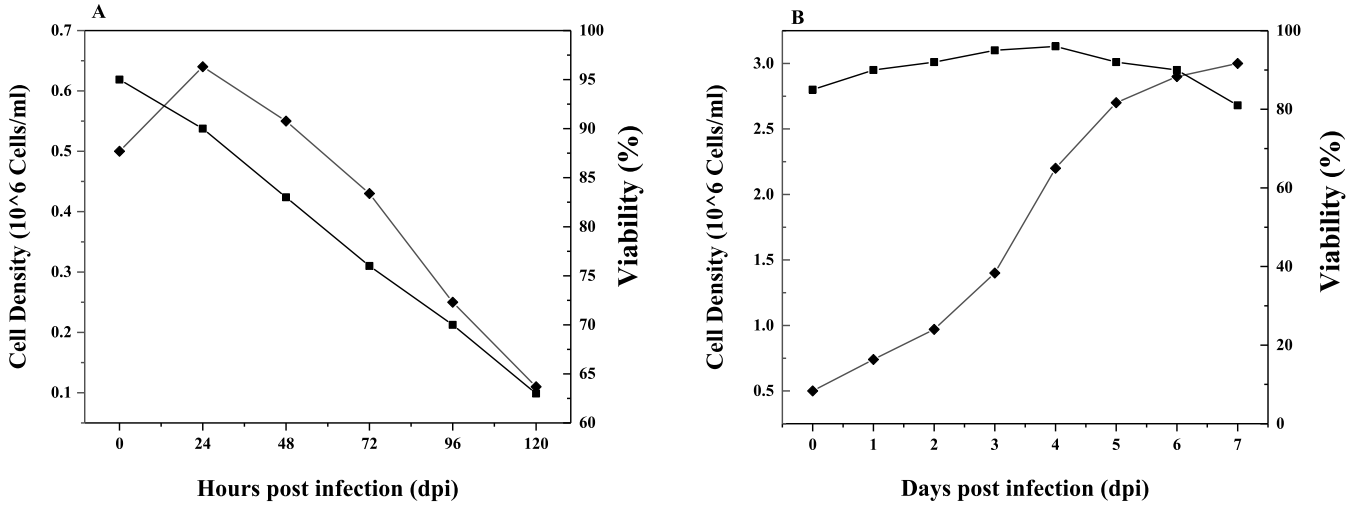

Figure 4. Effect of agitation speed and sparging on cell growth and viability in 200 L SUB. (A) Cell density and viability with high-speed agitation at RPM = 80 and sparging. (B) Cell density and viability with low-speed agitation RPM = 25 and without sparging (overlay system). ■: viability and ♦: VCD. All results are the mean values of triplicate data.

10^6 cells/mL, MOI = 9, and pH = 7.17 was confirmed in the shake flask in HEK 293 cells.[43] Other study demonstrated that with VCD up to 6−8 × 10^6 cells/mL at infection time, the virus titer up to 1−6 × 10^{10} viral particle/mL was obtained in the perfusion bioreactor manufacturing Ad26 with PER.C6 as the host cells.[44,45]

3.2. Effect of Different MOIs on rAd26 Manufacturing. The effect of infection at different MOIs = 3, 6, 9, 12, and 15 on cell growth rate and viability in the HEK 293 cells at initial VCD = 1.4 × 10^6 cells/mL with 95% viability is represented in Figures 2. The results in MOIs = 3 and 6 showed that the cells continued to grow even until 48 hpi, and only after that time, the cell growth started to decline. By looking at Figure 2B, it can be seen that viability even after 120 hpi is higher than 80% for MOI = 3 and is about 70% for MOI = 6. This result is in accordance with what Dill and Britio et al. obtained.[46,47] Dill et al. showed that decreasing MOI increased the viability and density of BHK cells infected with foot and mouth disease virus (FMDV).[46] As noted by Lavado-García et al. continued cell growth and no decrease in viability after infection could be related to the insufficient number of viruses to infect the host cell, so it can be understood that at MOIs = 3 and 6, the HEK 293 cells are not infected even after 120 hpi.[48]

Also, at MOI = 9, the cell density had a trend similar to MOIs = 3 and 6, so that in the time period of 0−48 hpi, the cell density increased and reached VCD = 2.0 × 10^6 cells/mL. However, according to Figure 2B, the viability shows its downward trend from 12 hpi and reaches approximately 45% at 84 hpi due to the virus replication and the lytic characteristics of the adenovirus. This behavior is different from the trend of changes in MOIs = 3 and 6. This result is in accordance with the finding of Nie et al.[43] that assessed three experimental CPPs (VCD, MOI, and virus production pH) by the design of experiment (DoE) method, and the robust set point of MOI = 9 was applied in both SFs and 2 L benchtop bioreactor. According to figures A and B, in MOIs = 12 and 15, cell growth has stopped since the first hours of infection, and the trend is downward. In other words, no cell growth was observed practically, so that at time 72 hpi of both experiments, the cell density decreased to less than 0.5 × 10^6 cells/mL and the viability decreased to below 40% in the same way. What can be inferred is that a premature cell death followed by cell lysis resulted in a considerable decrease in VCD, viability, and the effectiveness of infection.[29]

Figure 3 shows the rAd26 virus titer at different MOIs. According to this figure for MOIs = 3 and 6, the quantity of

https://doi.org/10.1021/acsomega.3c03007
ACS Omega 2023, 8, 36720−36728

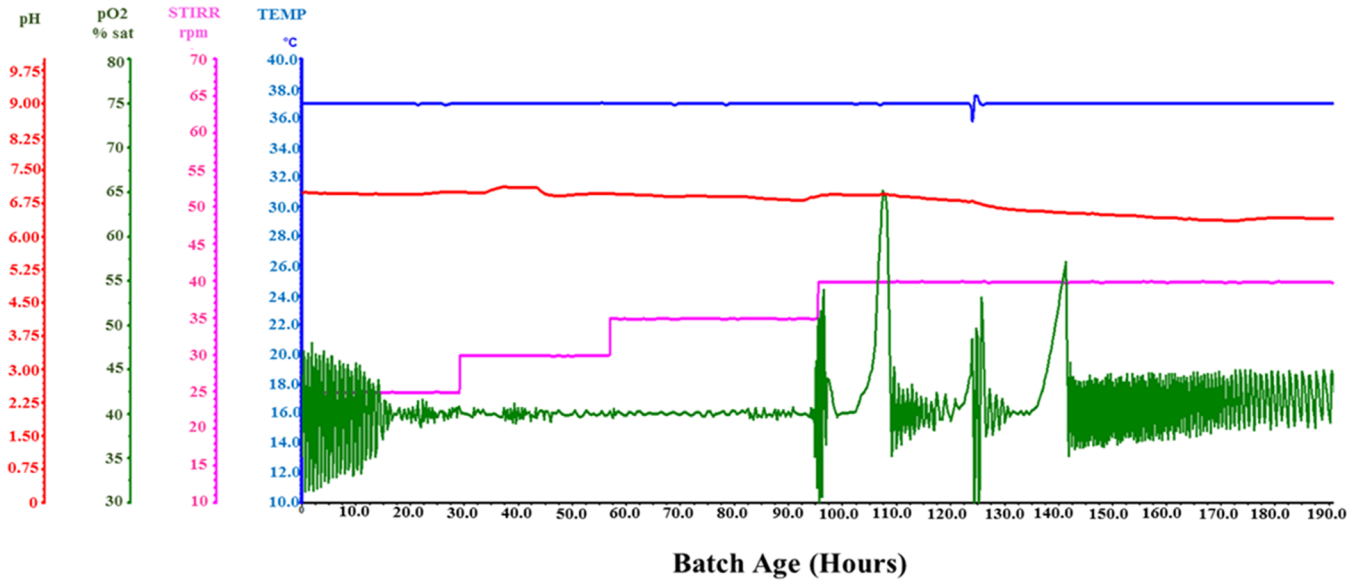

Figure 5. Online monitoring of the pH trend and infection in the 200 L stirred SUB. DO concentration was controlled using a cascade function with agitation rate and the addition of pure oxygen. The temperature was 37 °C, controlled automatically via the heater system. Once the cell density reached 1.4 ± 0.1 × 10^6 cells/mL on day 3, the cells were infected with the virus seed with MOI = 9.

adenovirus released in the supernatant (rAd26−S-CoV-2 replicated in HEK293 cell cultures), i.e., $TCID_{50}$/mL, was $10^{3.5}$ and $10^{6.1}$, respectively, at 72 hpi. These values are almost 10,000 and 100 times lower compared to the experiment infected at MOI = 9 ($TCID_{50}$/mL = $10^{8.8}$, at the same time). The results also revealed that infection with MOI = 9 provided a higher viral titer level rather than the infection with MOIs = 12 and 15. Likewise, other studies reported that the increase of MOI accelerated the cell death rate and even can cause the formation of defective interfering particles (DIPs), which may reduce the maximum achievable virus production.[49−51] Ferreira et al. designed two different processes for the manufacturing of the Ad26 vector as a COVID-19 vaccine, evaluated with SuperPro Designer software.[52] Their findings showed comparable results with our study, and a batch cell culture viral production made a viral titer of 10^9 viral particles (VP)/mL in both the stainless-steel (SS) and SUB. Furthermore, they performed perfusion cell culture viral manufacturing in the SUB, which resulted in a higher viral titer (1 × 10^{12} VP/mL) compared to the SS bioreactor with the same operating CPPs.[53]

3.3. Effect of Aeration on the Cell Growth in the 200 L Stirred SUB for the GMP Manufacturing Purpose. The HEK 293 cells are typically assumed as shear stress-sensitive cells to hydrodynamic stress.[54] They even become more sensitive to the environmental shear stress once they are infected by adenoviral particles due to the proteolytic nature of those kinds of viruses. Therefore, rAd GMP manufacturing is always a challenging issue to optimize the shear stress sensed by the infected cells. On the other hand, supplying the required nutrients for the cells through culture medium as well as the oxygen needed is done by agitation in stirred SUBs, which is inherently a shear stress creator.[54] Therefore, in this section for GMP and industrial-scale manufacturing of rAd26, this factor was examined in more detail. Figure 4A depicts the influence of the aeration system (sparging and agitation) on the HEK 293 cells growth rate, measured daily over 5 days of post-infection (dpi). The high-speed agitation (RPM = 80) with gas sparging resulted in the lowest VCD of HEK 293 cells. In fact by this strategy, at an early stage of the cell culture, the viability was dropped unpleasantly. Also, as Figure 4A shows, a considerable decrease in VCD was observed in a way that the cells could grow hardly for the first 24 h, and then, it was decreased considerably. What can be inferred from this result is that the decrease observed in cell density may be attributed to the environmental shear stress. Sensitivity to shear stress differs according to the cell line and cell size and could also be dependent on the intensity of shear stress (made by eddies in turbulent flow), pH, temperature, cell growth phase, and also the presence of antifoam and shear protectant agents such as Poloxamer 188 (often referred to as Pluronic F-68).[55] This is shown by the post-harvest cell counts in Figure 4A, which indicated that HEK 293 proliferation is quickly reduced at the high-speed agitation with sparging aeration. This is a result which confirmed the finding of Grein et al. declaring that the aeration system must be optimized and monitored to ensure the specific growth rate, for the production of oncolytic measles virus.[56] Also, Negrete et al. indicated that Pluronic F-68 concentrations ranging from 0.05 to 0.2% can be used in the culture of the suspension HEK 293 cells, as it did not display any adverse effect upon either VCD or viability. In the same way, the 5% CO_2 atmosphere in the overlay system was not restrictive for the cell growth of HEK 293 cells, while it reduced the growth rate using a sparger system.[57]

To address this issue and enhance the cell growth, the aeration system was investigated carefully using an overlay system, and the agitation rate was performed at low-speed conditions. As seen in Figure 4B, lowering the agitation speed to RPM = 25 increased the cell density and viability once the SUB was seeded at VCD = 0.4 × 10^6 cells/mL, with an overlay system. The VCD in the 200 L SUB was increased from 0.5 × 10^6 cells/mL to 1.4 × 10^6 cells/mL within 3 days (Figure 4B). After infection of the cells in the 200 L SUB, the cells grew exponentially over the next 24 h and reached VCD = 2.2 × 10^6 cells/mL and viability = 96%. After infection, cell growth arresting was observed while cell viability remained high only at 24 hpi, and after 185 hpi, the viability was decreased to 81%.

https://doi.org/10.1021/acsomega.3c03007
ACS Omega 2023, 8, 36720−36728

3.4. pH Trend after Infection in the 200 L SUB. The pH of medium was found to influence the titer of virus stocks, giving differences of up to 10^5 $TCID_{50}$ in result on infected HEK 293.[58] Online monitoring of pH in the 200 L SUB during batch mode cell culture with RPM = 25 agitation without sparging (overlay system) is presented in Figure 5. Online and offline recording of the pH fluctuation before infection revealed that the pH value fell from 7.2 to 7.0, and this is while the cell density was increased. According to the reported studies, uninfected cells typically entered the stationary phase at pH ∼ 6.9, which result in the decrease in cell growth. The rate of cell growth was found to be the same between 6.9 and 7.2 by comparing the pH at different days and different VCDs. The production of lactic acid, carbon dioxide, or ammonia by the cells is the reason for pH changes at this period of time.[47] However, continuous pH measurement taken during 72 hpi showed the decrease in pH. The lower pH is in fact the result of a decrease in oxygen consumption, cell death, and the release of rAd26 into the supernatant.[58] In most cases, after infection, viral replication within a cell alters the cell cycles, leading to cell death and an almost sharp pH drop to 6.5. In this study, cell growth decreased significantly at pH 6.8, as a result of virus infection-induced cell lysis. The effects of pH on E1- and E3-deleted recombinant adenovirus vector (rAV) production with HEK293S cells have been earlier studied by Jardon and Garnier, in the range of pH = 6.7−7.7.[59] They performed the experiments in a 4 mL × 500 mL bioreactor setup, and it was found that although the pH did not affect HEK 293 viability meaningfully, in the studied range, it had a significant effect on the virus titer and in very sharp optimum ranges.

The results obtained from the 200 L SUB demonstrated that the maximum virus titer occurred consistently at 72 hpi and the virus yield was strongly corresponding to the CPPs, such as cell density at infection, MOI, sparging/overlay aeration, and agitation speed. For the cells in the growth phase of batch culture, we may expect a stable but rapid reduction in pH and oxygen levels due to the rise in total biomass and cellular metabolism, as reported by Naciri et al. and other researchers.[60−62] It has been shown that the accumulation of some metabolic byproducts (such as ammonium, a result of glutamine metabolism) in batch culture can have a negative impact on cell growth and viability. Conversely, as glucose is consumed, lactate generation increases[63] at high lactate concentrations, the medium's ability to act as a buffer is reduced, and thus, the pH decreases, making the medium unfavorable for cell growth.[64−66]

4. CONCLUSIONS

In this study, we developed an optimized process for adenovirus vector vaccine GMP manufacturing using the one-factor-at-a-time (OFAT) technique to reduce process costs and to increase the viral titer. For this purpose, the cell culture process was initially optimized in 2 L shake flasks (SF 2 L) with batch mode operations using HEK 293 cells. The CPPs including VCD at ToI and MOI of adenovirus type 26 (rAd26) production were investigated by the OFAT approach, from which the optimal CPPs were obtained (VCD = 1.4 × 10^6 cells/ml and MOI = 9), yielding an adenovirus titer with $TCID_{50}$/mL = $10^{8.9}$, at 72 hpi. Finally, the optimal CPPs were experimentally scaled up and validated in the 50 L wave SUB and then in a 200 L SUB with low-speed agitation (RPM = 25) and without sparging (overlay system). The results in the 200 L SUB revealed that after infecting the HEK 293 host cells, their sensitivity (due to the proteolytic characteristics of the virus) to shear stress (made by the agitator and air bubbles from the sparger) increased, and in order to improve cell growth and to achieve a higher virus titer, different strategies need to be applied.

AUTHOR INFORMATION

Corresponding Author

Hossein Sedighikamal − *API Production Plant, Actoverco Biotech Company, Alborz 331325489, Iran; Division of Industrial Biotechnology, Department of Chemical Engineering, Sharif University of Technology, Tehran 11365-11155, Iran;* orcid.org/0000-0002-6720-9760; Phone: 98 26 347 60 314; Email: h.sedighikamal@che.sharif.edu

Authors

Alireza Sattarzadeh − *API Production Plant, Actoverco Biotech Company, Alborz 331325489, Iran*

Reza Karimi Mostofi − *API Production Plant, Actoverco Biotech Company, Alborz 331325489, Iran; Department of Pharmaceutics, Faculty of Pharmacy, Tehran University of Medical Sciences, Tehran 8741253641, Iran*

Behnoush Dinarvand − *API Production Plant, Actoverco Biotech Company, Alborz 331325489, Iran*

Madineh Nazarpour − *API Production Plant, Actoverco Biotech Company, Alborz 331325489, Iran*

Complete contact information is available at: https://pubs.acs.org/10.1021/acsomega.3c03007

Notes

The authors declare no competing financial interest.

ACKNOWLEDGMENTS

This work was a part of project code 303, which was supported financially by Actoverco Company, Iran. The authors are also grateful to the scientific staff of the Gamaleya Research Institute of Epidemiology and Microbiology, Russia.

REFERENCES

(1) Mohan, B.; Nambiar, V. COVID-19: an insight into SARS-CoV-2 pandemic originated at Wuhan City in Hubei Province of China. *J. Infect. Dis. Epidemiol.* **2020**, *6* (4), No. 146.

(2) Dong, Y.; Dai, T.; Wei, Y.; Zhang, L.; Zheng, M.; Zhou, F. A systematic review of SARS-CoV-2 vaccine candidates. *Signal Transduction Targeted Ther.* **2020**, *5* (1), No. 237.

(3) Dagotto, G.; Yu, J.; Barouch, D. H. Approaches and challenges in SARS-CoV-2 vaccine development. *Cell Host Microbe* **2020**, *28* (3), 364−370.

(4) Chen, W. H.; Strych, U.; Hotez, P. J.; Bottazzi, M. E. The SARS-CoV-2 vaccine pipeline: an overview. *Curr. Trop. Med. Rep.* **2020**, *7* (2), 61−64.

(5) Kiesslich, S.; Kamen, A. A. Vero cell upstream bioprocess development for the production of viral vectors and vaccines. *Biotechnol. Adv.* **2020**, *44*, No. 107608.

(6) Offersgaard, A.; Duarte Hernandez, C. R.; Pihl, A. F.; Costa, R.; Venkatesan, N. P.; Lin, X.; Van Pham, L.; Feng, S.; Fahnøe, U.; Scheel, T. K.; Ramirez, S.; et al. SARS-CoV-2 production in a scalable high cell density bioreactor. *Vaccines* **2021**, *9* (7), No. 706.

(7) Lemiale, F.; Haddada, H.; Nabel, G. J.; Brough, D. E.; King, C. R.; Gall, J. G. Novel adenovirus vaccine vectors based on the enteric-tropic serotype 41. *Vaccine* **2007**, *25* (11), 2074−2084.

(8) Jones, I.; Roy, P. Sputnik V COVID-19 vaccine candidate appears safe and effective. *Lancet* **2021**, *397* (10275), 642−643.

(9) Chavda, V. P.; Bezbaruah, R.; Valu, D.; Patel, B.; Kumar, A.; Prasad, S.; Kakoti, B. B.; Kaushik, A.; Jesawadawala, M. Adenoviral Vector-Based Vaccine Platform for COVID-19: Current Status. *Vaccines* **2023**, *11*, 432.
(10) Liu, X. M.; Liu, H.; Wu, B. C.; Li, S. C.; Ye, L. L.; Wang, Q. W.; Huang, P. T.; Chen, Z. L. Suspended aggregates as an immobilization mode for high-density perfusion culture of HEK 293 cells in a stirred tank bioreactor. *Appl. Microbiol. Biotechnol.* **2006**, *72*, 1144−1151.
(11) Sadoff, J.; Gray, G.; Vandebosch, A.; Cárdenas, V.; Shukarev, G.; Grinsztejn, B.; Douoguih, M.; et al. Safety and efficacy of single-dose Ad26. COV2. S vaccine against Covid-19. *N. Engl. J. Med.* **2021**, *384* (23), 2187−2201.
(12) Weaver, E. A.; Hillestad, M. L.; Khare, R.; Palmer, D.; Ng, P.; Barry, M. Characterization of species C human adenovirus serotype 6 (Ad6). *Virology* **2011**, *412* (1), 19−27.
(13) Vogels, R.; Zuijdgeest, D.; van Rijnsoever, R.; Hartkoorn, E.; Damen, I.; de Béthune, M. P.; Kostense, S.; Penders, G.; Helmus, N.; Koudstaal, W.; Cecchini, M.; et al. Replication-deficient human adenovirus type 35 vectors for gene transfer and vaccination: efficient human cell infection and bypass of preexisting adenovirus immunity. *J. Virol.* **2003**, *77* (15), 8263−8271.
(14) Ghaemmaghamian, Z.; Zarghami, R.; Walker, G.; O'Reilly, E.; Ziaee, A. Stabilizing vaccines via drying: Quality by design considerations. *Adv. Drug Delivery Rev.* **2022**, *187*, No. 114313.
(15) Balakrishnan, V. S. The arrival of Sputnik V. *Lancet Infect. Dis.* **2020**, *20* (10), 1128.
(16) Aboubakr, H. A.; Sharafeldin, T. A.; Goyal, S. M. Stability of SARS-CoV-2 and other coronaviruses in the environment and on common touch surfaces and the influence of climatic conditions: A review. *Transboundary Emerging Dis.* **2021**, *68* (2), 296−312.
(17) Chirico, F.; Teixeira da Silva, J. A.; Tsigaris, P.; Sharun, K. Safety & effectiveness of COVID-19 vaccines: A narrative review. *Indian J. Med. Res.* **2022**, *155* (1), 91−104.
(18) *COVID-19 Vaccine Implementation Analysis & Insights*; World Health Organization, 2022; pp 1−52.
(19) Krause, P.; Fleming, T. R.; Longini, I.; Henao-Restrepo, A. M.; Peto, R.; et al. COVID-19 vaccine trials should seek worthwhile efficacy. *Lancet* **2020**, *396* (10253), 741−743.
(20) Khoury, D. S.; Cromer, D.; Reynaldi, A.; Schlub, T. E.; Wheatley, A. K.; Juno, J. A.; et al. Neutralizing antibody levels are highly predictive of immune protection from symptomatic SARS-CoV-2 infection. *Nat. Med.* **2021**, *27* (7), 1205−1211.
(21) Chan, C.Y.-Y.; Tambyah, P. A. Preflucel: a Vero-cell culture-derived trivalent influenza vaccine. *Expert Rev. Vaccines* **2012**, *11* (7), 759−773.
(22) Gutiérrez-Granados, S.; Gòdia, F.; Cervera, L. Continuous manufacturing of viral particles. *Curr. Opin. Chem. Eng.* **2018**, *22*, 107−114.
(23) Teworte, S.; Malc1, K.; Walls, L. E.; Halim, M.; Rios-Solis, L. Recent advances in fed-batch microscale bioreactor design. *Biotechnol Adv.* **2022**, *55*, No. 107888.
(24) Jyothilekshmi, I.; Jayaprakash, N. Trends in monoclonal antibody production using various bioreactor systems. *J. Microbiol Biotechnol.* **2021**, *31* (3), 349−357.
(25) Wu, Y.; Bissinger, T.; Genzel, Y.; Liu, X.; Reichl, U.; Tan, W. S. High cell density perfusion process for high yield of influenza A virus production using MDCK suspension cells. *Appl. Microbiol. Biotechnol.* **2021**, *105*, 1421−1434.
(26) Leinonen, H. M.; Lipponen, E. M.; Valkama, A. J.; Hynynen, H.; Oruetxebarria, I.; Turkki, V.; Olsson, V.; Kurkipuro, J.; Samaranayake, H.; Määttä, A. M.; Parker, N. R.; et al. Preclinical proof-of-concept, analytical development, and commercial scale production of lentiviral vector in adherent cells. *Mol. Ther.–Methods Clin. Dev.* **2019**, *15*, 63−71.
(27) Valkama, A. J.; Oruetxebarria, I.; Lipponen, E. M.; Leinonen, H. M.; Käyhty, P.; Hynynen, H.; Turkki, V.; Malinen, J.; Miinalainen, T.; Heikura, T.; Parker, N. R.; et al. Development of large-scale downstream processing for lentiviral vectors. *Mol. Ther.–Methods Clin. Dev.* **2020**, *17*, 717−730.
(28) de Jongh, W. A.; Resende, M. D. S.; Leisted, C.; Strøbæk, A.; Berisha, B.; Nielsen, M. A.; Salanti, A.; Hjerrild, K.; Draper, S.; Dyring, C. Development of a Drosophila S2 insect-cell based placental malaria vaccine production process. *BMC Proc.* **2013**, *7* (6), 20.
(29) Milián, E.; Kamen, A. A. Current and emerging cell culture manufacturing technologies for influenza vaccines. *BioMed. Res. Int.* **2015**, *2015*, No. 504831.
(30) Petiot, E.; Cuperlovic-Culf, M.; Shen, C. F.; Kamen, A. Influence of HEK293 metabolism on the production of viral vectors and vaccine. *Vaccine* **2015**, *33*, 5974−5981.
(31) Tripathi, N. K.; Shrivastava, A. Recent developments in bioprocessing of recombinant proteins: Expression hosts and process development. *Front. Bioeng. Biotechnol.* **2019**, *7*, 420.
(32) Tan, E.; Chin, C. S. H.; Lim, Z. F. S.; Ng, S. K. HEK293 cell line as a platform to produce recombinant proteins and viral vectors. *Front. Bioeng. Biotechnol.* **2021**, *9*, No. 796991.
(33) Jang, M.; Pete, E. S.; Bruheim, P. The impact of serum-free culture on HEK293 cells: From the establishment of suspension and adherent serum-free adaptation cultures to the investigation of growth and metabolic profiles. *Front. Bioeng. Biotechnol.* **2022**, *10*, No. 964397.
(34) Iyer, P.; Ostrove, J. M.; Vacante, D. Comparison of manufacturing techniques for adenovirus production. *Cytotechnology* **1999**, *30*, 169−172.
(35) Park, S.; Kim, J. Y.; Ryu, K. H.; Kim, A. Y.; Kim, J.; Ko, Y. J.; Lee, E. G. Production of a foot-and-mouth disease vaccine antigen using suspension-adapted BHK-21 cells in a bioreactor. *Vaccines* **2021**, *9* (5), 505.
(36) Nadeau, I.; Kamen, A. Production of adenovirus vector for gene therapy. *Biotechnol. Adv.* **2003**, *20* (7−8), 475−489.
(37) Ferreira, T. B.; Ferreira, A. L.; Carrondo, M. J. T.; Alves, P. M. Effect of refeed strategies and non-ammoniagenic medium on adenovirus production at high cell densities. *J. Biotechnol.* **2005**, *119* (3), 272−280.
(38) Fedosyuk, S.; Merritt, T.; Peralta-Alvarez, M. P.; Morris, S. J.; Lam, A.; Laroudie, N.; Kangokar, A.; Wright, D.; Warimwe, G. M.; Angell-Manning, P.; Ritchie, A. J.; et al. Simian adenovirus vector production for early-phase clinical trials: A simple method applicable to multiple serotypes and using entirely disposable product-contact components. *Vaccine* **2019**, *37* (47), 6951−6961.
(39) Keiser, P. T.; Anantpadma, M.; Staples, H.; Carrion, R.; Davey, R. A. Automation of infectious focus assay for determination of filovirus titers and direct comparison to plaque and TCID50 assays. *Microorganisms* **2021**, *9* (1), 156.
(40) Smither, S. J.; Lear-Rooney, C.; Biggins, J.; Pettitt, J.; Lever, M. S.; Olinger, J.; GG. Comparison of the plaque assay and 50% tissue culture infectious dose assay as methods for measuring filovirus infectivity. *J. Virol. Methods* **2013**, *193* (2), 565−571.
(41) Wulff, N. H.; Tzatzaris, M.; Young, P. J. Monte carlo simulation of the spearman-kaerber TCID50. *J. Clin. Bioinf.* **2012**, *2* (1), No. 5.
(42) SAS, S. *STAT Software*, version 9.1; SAS Institute Inc.: Cary, NC USA, 2002.
(43) Nie, J.; Sun, Y.; Feng, K.; Huang, L.; Li, Y.; Bai, Z. The efficient development of a novel recombinant adenovirus zoster vaccine perfusion production process. *Vaccine* **2022**, *40* (13), 2036−2043.
(44) Henry, O.; Dormond, E.; Perrier, M.; Kamen, A. Insights into adenoviral vector production kinetics in acoustic filter-based perfusion cultures. *Biotechnol. Bioeng.* **2004**, *86* (7), 765−774.
(45) Cortin, V.; Thibault, J.; Jacob, D.; Garnier, A. High-titer adenovirus vector production in 293S cell perfusion culture. *Biotechnol. Prog.* **2004**, *20* (3), 858−863.
(46) Dill, V.; Ehret, J.; Zimmer, A.; Beer, M.; Eschbaumer, M. Cell Density Effects in Different Cell Culture Media and Their Impact on the Propagation of Foot-And-Mouth Disease Virus. *Viruses* **2019**, *11*, 511.
(47) Brito, B. P.; Rodriguez, L. L.; Hammond, J. M.; Pinto, J.; Perez, A. M. Review of the Global Distribution of Foot-and-Mouth Disease Virus from 2007 to 2014. *Transbound. Emerg. Dis.* **2017**, *64*, 316−332.

https://doi.org/10.1021/acsomega.3c03007
ACS Omega 2023, 8, 36720−36728

(48) Lavado-García, J.; Pérez-Rubio, P.; Cervera, L.; Gòdia, F. The cell density effect in animal cell-based bioprocessing: Questions, insights and perspectives. *Biotechnol. Adv.* **2022**, *60*, No. 108017.
(49) Frensing, T. Defective interfering viruses and their impact on vaccines and viral vectors. *Biotechnology journal* **2015**, *10* (5), 681−689.
(50) Sun, Y.; Huang, L.; Nie, J.; Feng, K.; Liu, Y.; Bai, Z. Development of a perfusion process for serum-free adenovirus vector herpes zoster vaccine production. *AMB Express* **2022**, *12* (1), No. 58.
(51) Nienow, A. W. Reactor engineering in large scale animal cell culture. *Cytotechnology* **2006**, *50* (1−3), 9.
(52) Ferreira, R. G.; Gordon, N. F.; Stock, R.; Petrides, D. Adenoviral Vector COVID-19 Vaccines: Process and Cost Analysis. *Processes* **2021**, *9*, 1430.
(53) Custers, J.; Kim, D.; Leyssen, M.; Gurwith, M.; Tomaka, F.; Robertson, J.; Heijnen, E.; Condit, R.; Shukarev, G.; Heerwegh, D.; van Heesbeen, R.; Schuitemaker, H.; Douoguih, M.; Evans, E.; Smith, E. R.; Chen, R. T.; Brighton Collaboration Viral Vector Vaccines Safety Working Group (V3SWG). Vaccines based on replication incompetent Ad26 viral vectors: Standardized template with key considerations for a risk/benefit assessment. *Vaccine* **2021**, *39* (22), 3081−3101.
(54) Seidel, S.; Maschke, R. W.; Mozaffari, F.; Eibl-Schindler, R.; Eibl, D. Improvement of HEK293 Cell Growth by Adapting Hydrodynamic Stress and Predicting Cell Aggregate Size Distribution. *Bioengineering* **2023**, *10* (4), 478.
(55) van der Pol, L.; Tramper, J. Shear sensitivity of animal cells from a culture-medium perspective. *Trends Biotechnol.* **1998**, *16* (8), 323−328.
(56) Grein, T. A.; Loewe, D.; Dieken, H.; Weidner, T.; Salzig, D.; Czermak, P. Aeration and shear stress are critical process parameters for the production of oncolytic measles virus. *Front. Bioeng. Biotechnol.* **2019**, *7*, No. 78.
(57) Negrete, A.; Ling, T. C.; Lyddiatt, A. Effect of Pluronic F-68, 5% CO, Atmosphere, HEPES, and Antibiotic-Antimycotic on Suspension Adapted 293 Cells. *Open Biotech. J.* **2008**, *2*, 229−234.
(58) Johnson, F. B.; Bodily, A. S. Effect of environmental pH on adenovirus-associated virus. *Proc. Soc. Exp Biol. Med.* **1975**, *150* (3), 585−590.
(59) Jardon, M.; Garnier, A. PH, pCO2, and temperature effect on R-adenovirus production. *Biotechnol. Prog.* **2003**, *19* (1), 202−208.
(60) Genzel, Y.; Vogel, T.; Buck, J.; Behrendt, I.; Ramirez, D. V.; Schiedner, G.; Jordan, I.; Reichl, U. High cell density cultivations by alternating tangential flow (ATF) perfusion for influenza A virus production using suspension cells. *Vaccine* **2014**, *32* (24), 2770−2781.
(61) McQueen, A.; Bailey, J. E. Effect of ammonium ion and extracellular pH on hybridoma cell metabolism and antibody production. *Biotechnol. Bioeng.* **1990**, *35* (11), 1067−1077.
(62) Naciri, M.; Kuystermans, D.; Al-Rubeai, M. Monitoring pH and dissolved oxygen in mammalian cell culture using optical sensors. *Cytotechnology* **2008**, *57*, 245−250.
(63) Mirabet, M.; Navarro, A.; Lopez, A.; Canela, E. I.; Mallol, J.; Lluis, C.; Franco, R. Ammonium toxicity in different cell lines. *Biotechnol. Bioeng.* **1997**, *56* (5), 530−537.
(64) Reinhart, D.; Damjanovic, L.; Castan, A.; Ernst, W.; Kunert, R. Differential gene expression of a feed-spiked super-producing CHO cell line. *J. Biotechnol.* **2018**, *285*, 23−37.
(65) Chen, K.; Liu, Q.; Xie, L.; Sharp, P. A.; Wang, D. I. Engineering of a mammalian cell line for reduction of lactate formation and high monoclonal antibody production. *Biotechnol. Bioeng.* **2001**, *72* (1), 55−61.
(66) Sedighikamal, H.; Karimi Mostofi, R.; Sattarzadeh, A.; Shahbazi, M.; Aghazadeh, H. Comparative study of commercial media to improve GMP manufacturing of recombinant human interferon β-1a by CHO cells in perfusion bioreactor. *Cytotechnology* **2022**, *74* (6), 669−680.

https://doi.org/10.1021/acsomega.3c03007
ACS Omega 2023, 8, 36720−36728